SUPPLEMENTAL VIDEO, TABLE

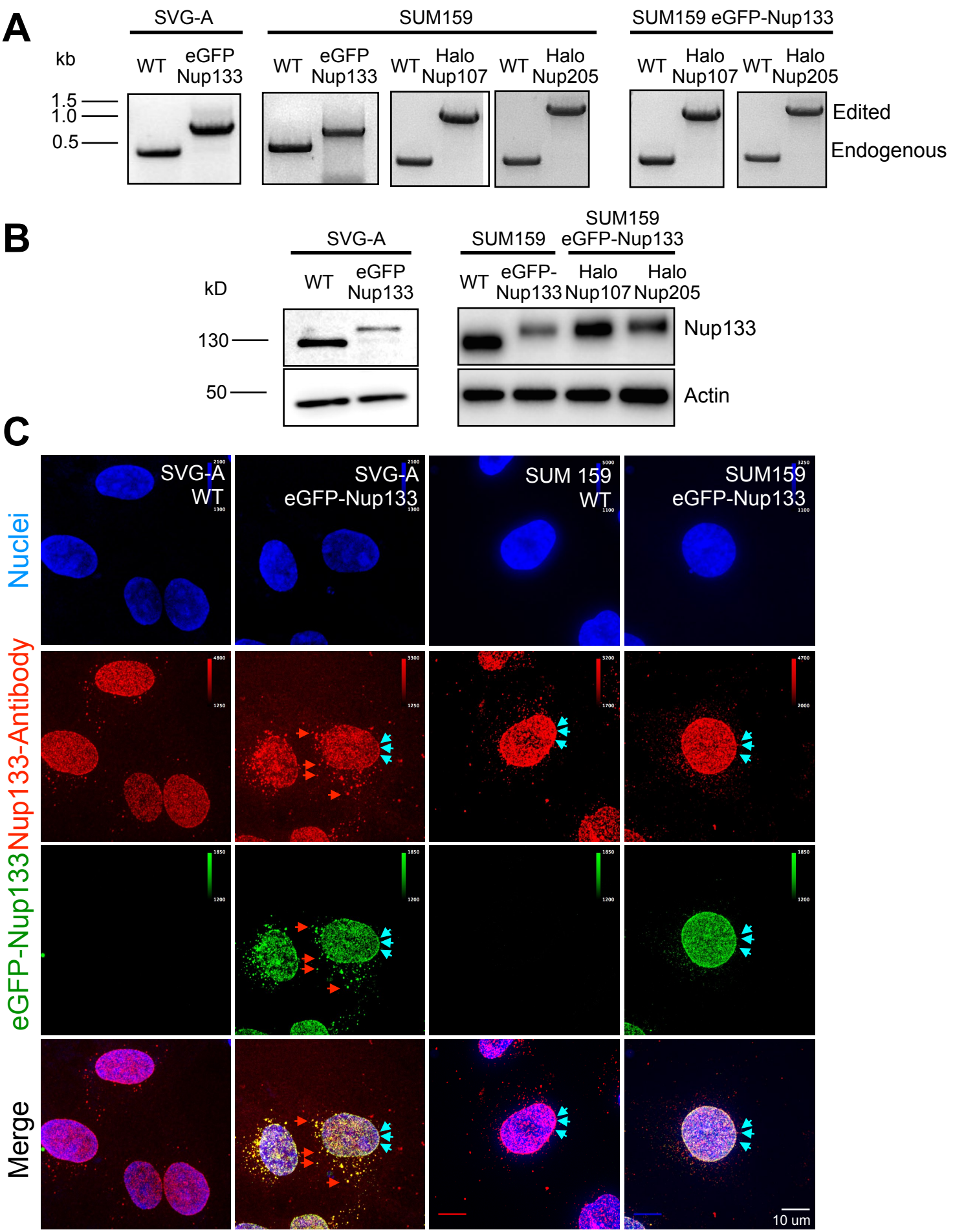
A
SVG-A
SUM159
SUM159 eGFP-Nup133
kb
WT
eGFP Nup133
WT
eGFP Nup133
WT
Halo Nup107
WT
Halo Nup205
WT
Halo Nup107
WT
Halo Nup205
1.5
1.0
0.5
Edited
Endogenous
B
SVG-A
SUM159
SUM159 eGFP-Nup133
kD
WT
eGFP Nup133
WT
eGFP-Nup133
Halo Nup107
Halo Nup205
130
50
Nup133
Actin
C
Nuclei
eGFP-Nup133Nup133-Antibody
Merge
SVG-A WT
SVG-A eGFP-Nup133
SUM 159 WT
SUM159 eGFP-Nup133
10 um

Figure S1. Characterization of genome-edited SUM159 and SVG-A cells, Related to Figure 1.

(A) Genomic PCR analysis demonstrating biallelic integration of eGFP or Halo sequences into the Nup107, Nup133 or Nup205 locus in genome-edited cell lines from SVG-A or SUM159 cells. The single PCR products obtained using the same set of probes were smaller in the parental cells (WT) than the corresponding product obtained from the genome-edited cell lines. Position and size of DNA molecular weight markers are shown.

(B) Western blot analysis with a rabbit monoclonal antibody specific for Nup133 of SVG-A and SUM159 cells demonstrating full replacement of the endogenous protein with the chimera in SVG-A and SUM159 cells; actin was used as gel-lane loading control. Position and size of protein molecular weight markers are shown.

(C) xy-projections along the optical axis of images obtained using spinning disc confocal microscopy during interphase of chemically fixed parental WT or genome-edited SVG-A and SUM159 cells expressing eGFP-Nup133. Staining with a rabbit monoclonal antibody specific for Nup133 highlights the location of Nup133 at the nuclear envelope (cyan arrows) and volume excluded by the nucleus (red arrows); the nucleus was identified using DAPI. Scale bar, 10 um.

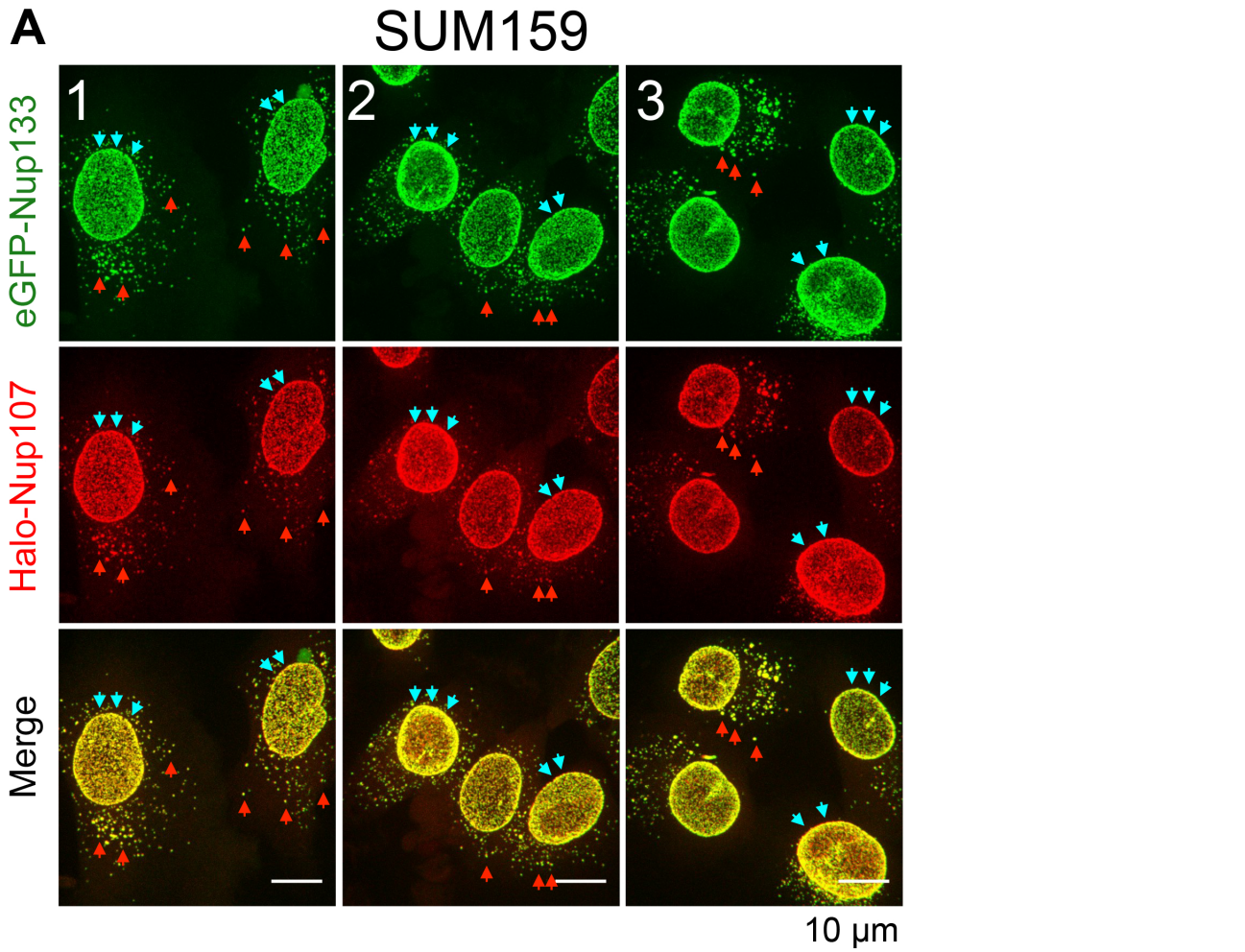
A
SUM159
eGFP-Nup133
Halo-Nup107
Merge
1
2
3
10 μm

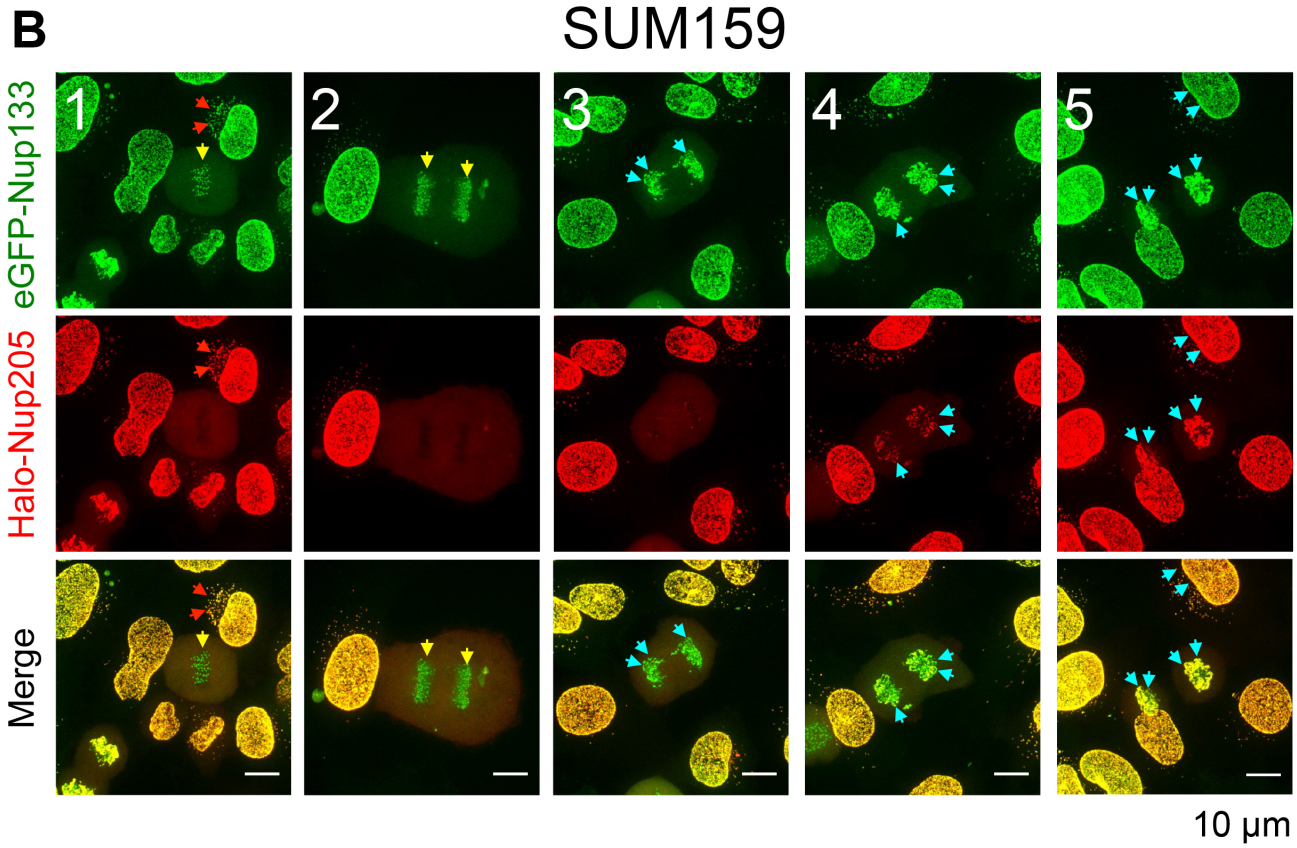
B
SUM159
eGFP-Nup133
Halo-Nup205
Merge
1
2
3
4
5
10 μm

Figure S2. eGFP-Nup133, Halo-Nup107 and Halo-Nup205 colocalize in the nuclear envelope of genome-edited SUM159 cells, Related to Figure 2.

(A) Representative snapshots from three examples of xy-projections along the optical axis of images obtained by spinning disc confocal microscopy of double genome-edited SUM159 cells expressing eGFP-Nup133 and Halo-Nup107 visualized during interphase. Halo-Nup107 was fluorescently labeled by brief incubation of the cells with Janelia Flour ® 549. Arrowheads highlight spots located in nuclear envelope (cyan) and the cytosolic volume (red). Scale bars, 10 um.

(B) Representative snapshots from five examples corresponding to xy-projections along the optical axis obtained by spinning disc confocal microscopy of five double genome-edited SUM159 cells expressing eGFP-Nup133 together with Halo-Nup205 imaged during cell division. Halo-Nup205 was fluorescently labeled with Janelia Flour ® 549 by brief incubation of the cells with the dye. Arrowheads highlight eGFP-Nup133 spots located in the kinetochores (yellow) during mitosis; as expected, Halo-Nup205 was absent. Arrowheads (cyan) indicate locations of eGFP-Nup133 and Halo-Nup205 in the nuclear envelope of the highlighted cells imaged towards the end of cell division or during interphase. Arrowheads (red) indicate location of eGFP-Nup133 and Halo-Nup205 in cytosol of a cell during interphase. Scale bars, 10 um.

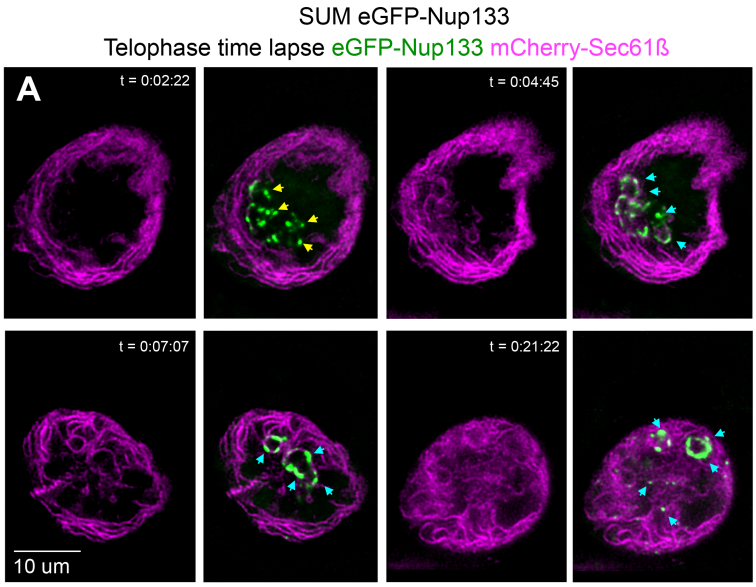
SUM eGFP-Nup133
Telophase time lapse eGFP-Nup133 mCherry-Sec61ß
A
t = 0:02:22
t = 0:04:45
t = 0:07:07
t = 0:21:22
10 um

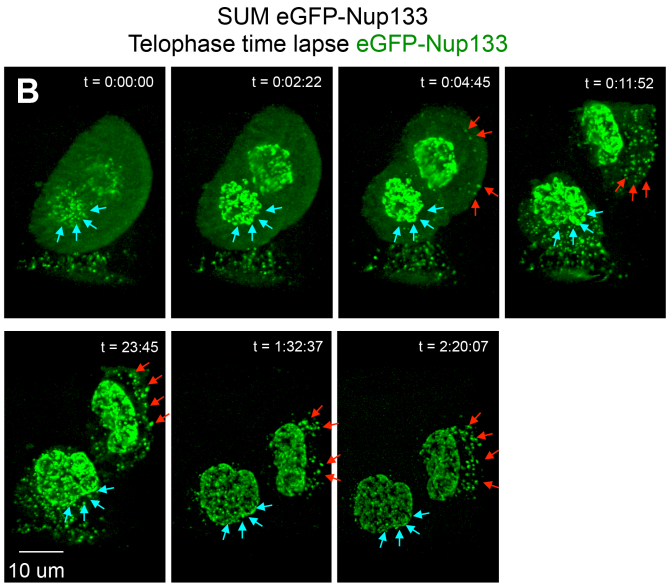
SUM eGFP-Nup133
Telophase time lapse eGFP-Nup133
B
t = 0:00:00
t = 0:02:22
t = 0:04:45
t = 0:11:52
t = 23:45
t = 1:32:37
t = 2:20:07
10 um

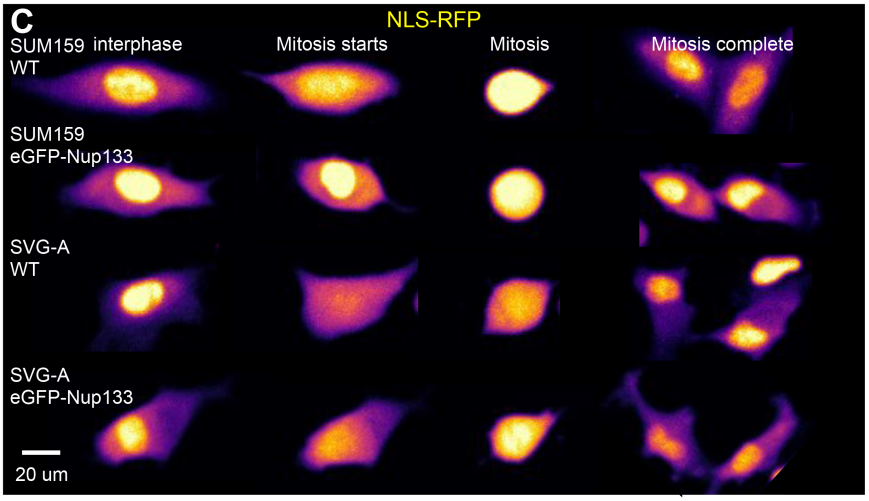
C
NLS-RFP
SUM159 interphase
Mitosis starts
Mitosis
Mitosis complete
WT
SUM159
eGFP-Nup133
SVG-A
WT
SVG-A
eGFP-Nup133
20 um

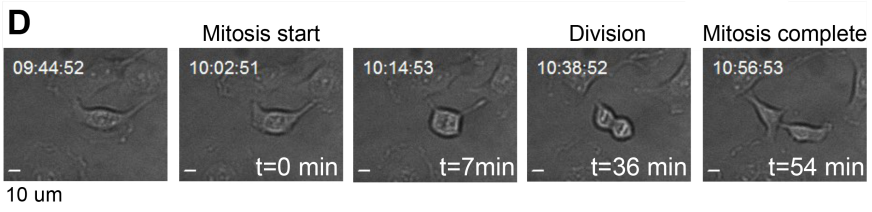
D
Mitosis start
Division
Mitosis complete
09:44:52
10:02:51
10:14:53
10:38:52
10:56:53
t=0 min
t=7min
t=36 min
t=54 min
10 um

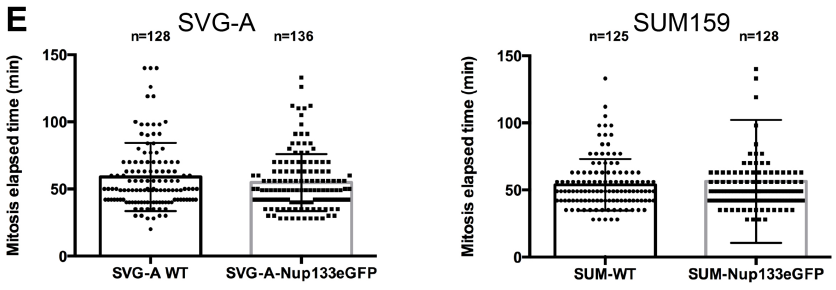
E
SVG-A
n=128
n=136
Mitosis elapsed time (min)
150
100
50
0
SVG-A WT
SVG-A-Nup133eGFP
SUM159
n=125
n=128
SUM-WT
SUM-Nup133eGFP

Figure S3. Distribution of Nup133 and nuclear import of NLS-RFP during cell division, Related to Figure 1.

(A) Selected single optical sections from images obtained using LLSM of live genome-edited SUM159 cells expressing eGFP-Nup133 (green) at different stages during telophase. The ER and newly forming nuclear envelope are marked by ectopic expression of mCherry-Sec61β (purple). The representative images illustrate the early association of eGFP-Nup133 with mCherry-Sec61β in the non-core region of the nascent nuclear envelope (cyan arrows); association of eGFP-Nup133 with kinetochores is highlighted with yellow arrows. Time stamps are relative to the start of the time series. Scale bar, 10 um.

(B) Volumetric projections from sequential images of a time series during cytokinesis obtained using spinning disk confocal fluorescence microscopy highlighting the association of eGFP-Nup133 with the nuclear envelope (cyan and emergence of bright spots (red) in the cytosolic non-nuclear volume during late stages of telophase. Time stamps are relative to the start of the time series. Scale bar, 10 um.

(C) Maximum projection along the z-axis from images acquired using spinning disc confocal microscopy of parental and genome-edited SUM159 and SVG-A cells expressing eGFP-Nup133 together with ectopic expression of NLS-RFP during different stages of cell division. The representative images show the nuclear localization of NLS-RFP during interphase, its cytosolic distribution during mitosis, and its post mitotic nuclear import upon completion of cell division. Scale bar, 20 um.

(D) Elapsed time required for cell division for genome-edited SVG-A cells expressing eGFP-Nup133 determined from time series acquired using wide field phase contrast microscopy. The elapsed time was approximated as the interval between the onset of cell rounding (t=0 min) and the separation of the two daughter cells. Scale bar, 10 um.

(E) Dot plots summarizing elapsed time results for genome-edited SUM and SVG-A cells from two independent biological experiments (n= number of cells). There was no statistically significant difference between the elapsed times of parental and genome-edited cells as determined by Mann-Whitney ($p = 0.2492$) or unpaired t tests ($p = 0.1481$).

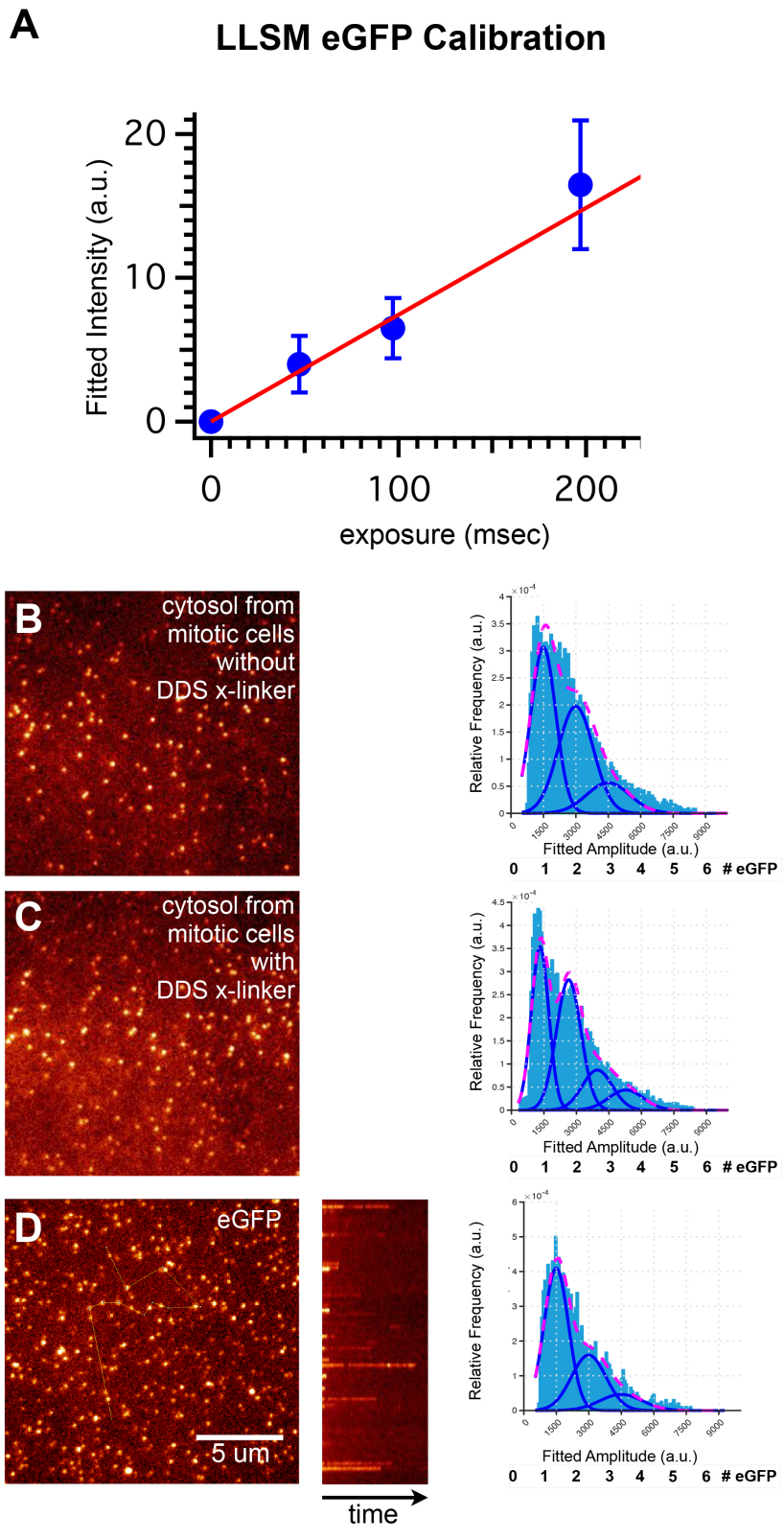
A
LLSM eGFP Calibration
Fitted Intensity (a.u.)
20
10
0
0
100
200
exposure (msec)
B
cytosol from mitotic cells without DDS x-linker
C
cytosol from mitotic cells with DDS x-linker
D
eGFP
5 um
time
Relative Frequency (a.u.)
Fitted Amplitude (a.u.)
0 1 2 3 4 5 6 # eGFP

Figure S4. Single-molecule imaging of eGFP, Related to Figure 1.
(A) Single-molecule calibration of eGFP fluorescence intensity using LLSM. Recombinant eGFPs isolated from *E. coli* were adsorbed at low surface density to a freshly glow discharged glass coverslip and illuminated continuously with LLSM. The plot is from background-corrected fluorescence intensities corresponding to single-step bleaching events from diffraction-limited fluorescent spots acquired with the sCMOS camera at the different exposures used for all the experiments. Data is the fitted mean ± standard deviation.
(B,C) Single TIRF snapshots from cytosol isolated from genome-edited SUM159 cells during mitosis expressing eGFP-Nup133 without (**B**) or with (**C**) incubation of the cells with DSS, a membrane-permeable crosslinker prior to cell lysis. The histograms represent distributions of fluorescence intensity determined from diffraction-limited spots within the snapshot. The fit corresponds to linear combinations of normal distributions; the most prominent, centered at 1497 ± 564 (n= 12308; without crosslinker) and 1321 ± 401 (n= 12894; with crosslinker), show the intensity of a single eGFP.
(D) Single-molecule calibration of eGFP fluorescence intensity using TIRF. Snapshot from a time series and corresponding kymograph, obtained by continuous TIRF illumination with 200 ms exposures, of recombinant eGFP purified from *E. coli* adsorbed to a glass coverslip. The kymograph illustrates the occurrence of bleaching steps from diffraction-limited spots, and the histogram represents the distribution of florescence intensity associated with the single bleaching steps. The fit corresponds to linear combinations of normal distributions; the most prominent, centered at 1497 ± 574 (mean ± SD; n= 2799), show the fluorescence intensity of a single eGFP molecule. Scale bar, 10 um.

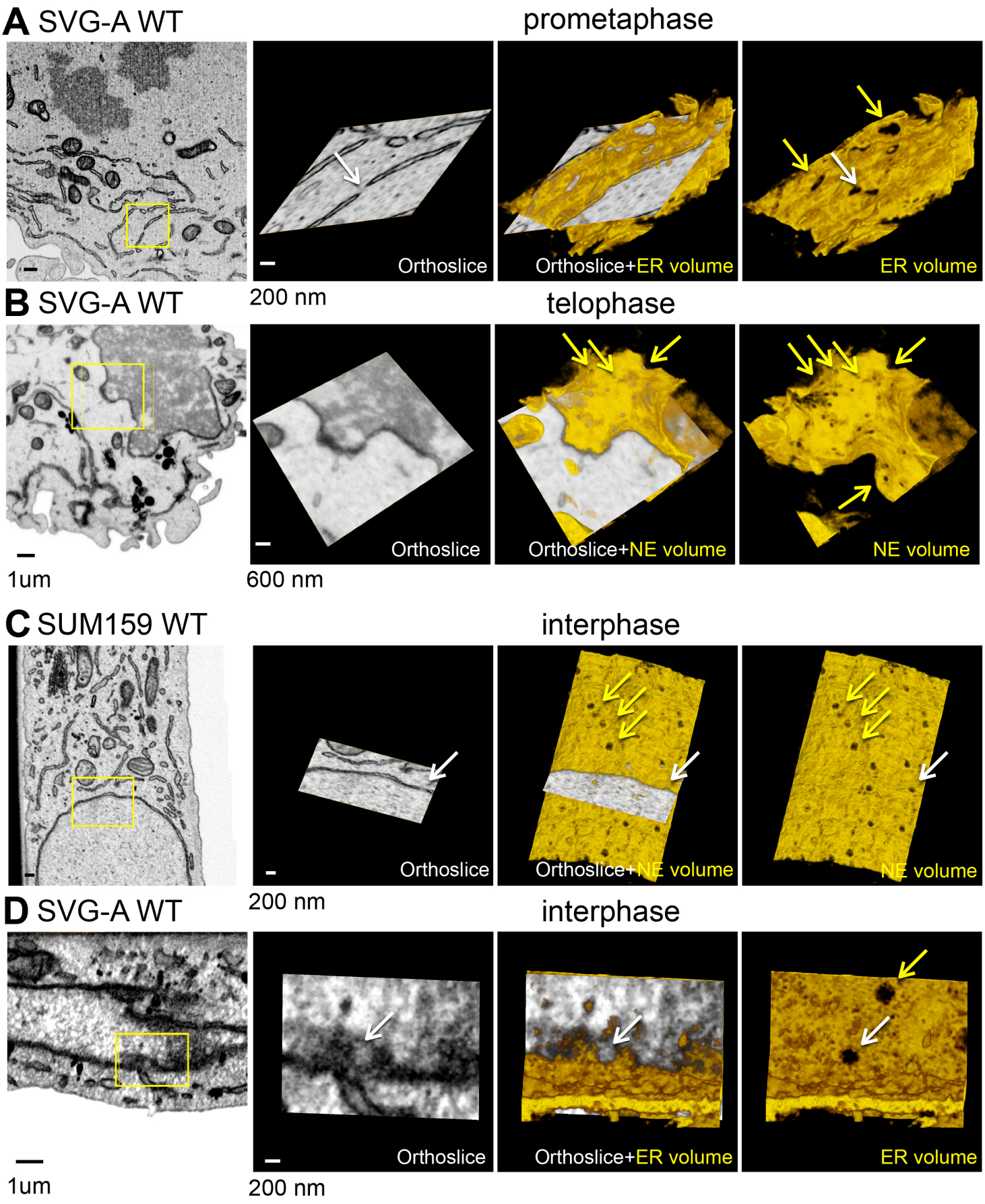
A SVG-A WT
prometaphase
Orthoslice
Orthoslice+ER volume
ER volume
200 nm
B SVG-A WT
telophase
Orthoslice
Orthoslice+NE volume
NE volume
1um
600 nm
C SUM159 WT
interphase
Orthoslice
Orthoslice+NE volume
NE volume
200 nm
D SVG-A WT
interphase
Orthoslice
Orthoslice+ER volume
ER volume
1um
200 nm

Figure S5. Ultrastructure of nuclear envelope and ER sheets at different stages during the cell cycle imaged with 3D FIB-SEM, Related to Figures 5 and 6.
Imaging with volumetric 3D FIB-SEM illustrates the appearance of the nuclear envelope and the ER at different stages of cell division. The enlarged views of parental SUM159 and SVG-A cells show selected orthoslices and segmented membranes within the associated volume. The yellow arrows point to nuclear pores and fenestrations within the segmented membranes; the white arrows point to nuclear pores and fenestrations at the intersection of the orthoslice and the segmented membrane. Scale bars, 200 nm, 600 nm and 1 um.
(A) Parental SVG-A cell during prometaphase showing a representative example of a cross section containing ER sheets. The highlighted region depicts an example of a fenestrated ER sheet. The cell was scored as prometaphase because its chromatin was less condensed than in metaphase. Scale bars, 200 nm.
(B) Parental SVG-A cell during telophase showing a region of nuclear envelope containing newly formed post-mitotic nuclear pores. The yellow arrows point to nuclear pores within the segmented membrane. Scale bars, 600 nm and 1 um.
(C) Parental SUM159 cell during interphase showing a region of nuclear envelope containing nuclear pores. Scale bars, 200 nm.
(D) Parental SVG-A cell during interphase showing an ER sheet region contiguous to a nuclear envelope containing nuclear pores. Scale bars, 200 nm.

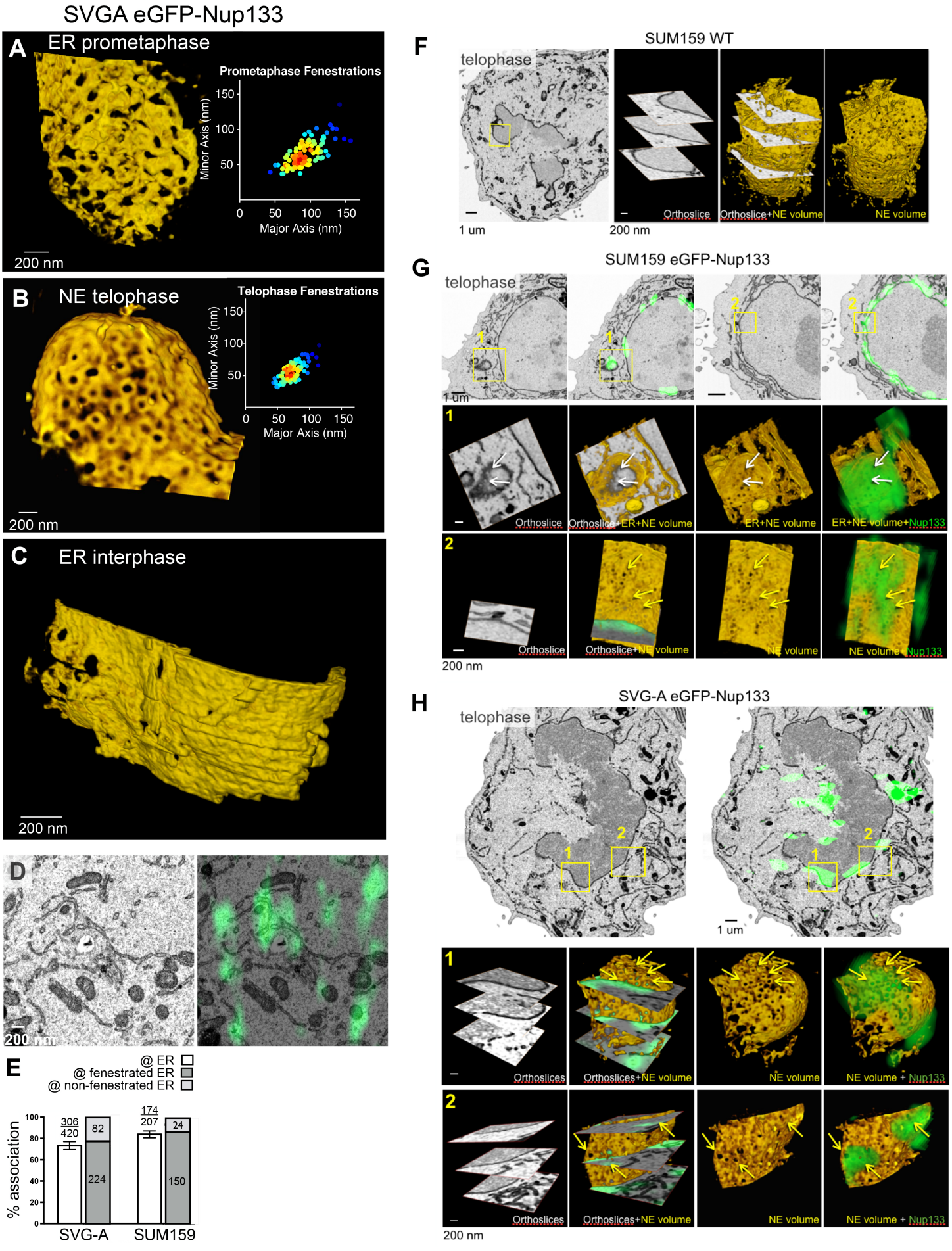
SVGA eGFP-Nup133
A
ER prometaphase
Prometaphase Fenestrations
Minor Axis (nm)
Major Axis (nm)
200 nm
B
NE telophase
Telophase Fenestrations
200 nm
C
ER interphase
200 nm
D
200 nm
E
@ ER
@ fenestrated ER
@ non-fenestrated ER
% association
306
420
82
224
174
207
24
150
SVG-A
SUM159
F
SUM159 WT
telophase
1 um
200 nm
Orthoslice
Orthoslice+NE volume
NE volume
G
SUM159 eGFP-Nup133
telophase
1 um
Orthoslice
Orthoslice+ER+NE volume
ER+NE volume
ER+NE volume+Nup133
Orthoslice+NE volume
NE volume
NE volume+Nup133
200 nm
H
SVG-A eGFP-Nup133
telophase
1 um
Orthoslices
Orthoslices+NE volume
NE volume
NE volume + Nup133
200 nm

Figure S6. Ultrastructure of nuclear envelope and mitotic ER sheets at different stages of the cell cycle imaged with 3D FIB-SEM, Related to Figures 5 and 6.
Representative imaging with 3D FIB-SEM illustrates the appearance of a fenestrated ER sheet during prometaphase, a non-fenestrated ER sheet during interphase, and the nuclear envelope during late telophase of different genome-edited SVG-A cells expressing eGFP-Nup133 together with stable ectopic expression of mCherry-Sec61β. Scale bars, 200 nm.
(A) Example of fenestrations within the segmented ER membrane from a cell imaged during prometaphase. The dots in the plot show the orthogonal dimensions of relatively heterogeneous single fenestrations color-coded for their relative abundance.
(B) Example of fenestrations within the inner region of a post mitotic nuclear envelope from a cell imaged during telophase. The dots in the plot show the orthogonal dimensions of relatively homogeneous single fenestrations color-coded for their relative abundance.
(C) Example of ER mostly devoid of fenestrations from a cell imaged during interphase.
(D) Orthoslice from correlative 3D spinning disc confocal fluorescence imaging with FIB-SEM-CLEM illustrates the colocalization of fluorescence from eGFP-Nup133 spots (green) with ER sheets during prometaphase in genome-edited SVG-A cells expressing eGFP-Nup133. Scale bars, 200 nm.
(E) Extent of eGFP-Nup133 colocalization with ER, enriched or not enriched in fenestrations, in genome edited SVG-A and SUM159 cells expressing eGFP-Nup133. Data for each cell type are from three different FIB-SEM volumes of 80-110 um^3; they illustrate the significant degree of overlap with local regions of ER sheets displaying fenestrations. Numbers of fluorescent spots within the fenestrated ER and with the ER within the imaged volume are indicated.
(F) 3D FIB-SEM in a parental SUM159 cell during telophase illustrates abundance of homogeneous fenestrations in the none-core region of the nuclear envelope. Enlarged view is from boxed region. Scale bars, 1 um and 200 nm.
(G) Correlative 3D spinning disc confocal fluorescence imaging with FIB-SEM-CLEM of a genome-edited SUM159 cell during telophase expressing eGFP-Nup133 illustrates the colocalization of fluorescence (green) from eGFP-Nup133 with homogeneous fenestrations in the non-core region of the nuclear envelope. Enlarged views are from boxed regions. The yellow arrows point to fenestrations within the non-core region of the nuclear envelope; the white arrows highlight fenestrations at the intersection of the orthoslice and the segmented membrane. Scale bars, 1 um and 200 nm.
(H) Correlative 3D spinning disc confocal fluorescence imaging with FIB-SEM-CLEM of a genome-edited SVG-A cell expressing eGFP-Nup133 during telophase illustrates the colocalization of fluorescence (green) from eGFP-Nup133 with homogeneous fenestrations in the non-core region of the nuclear envelope. Enlarged views are from boxed regions. The yellow arrows point to homogenous fenestrations within the non-core region of the nuclear envelope. Scale bars, 1 um and 200 nm.

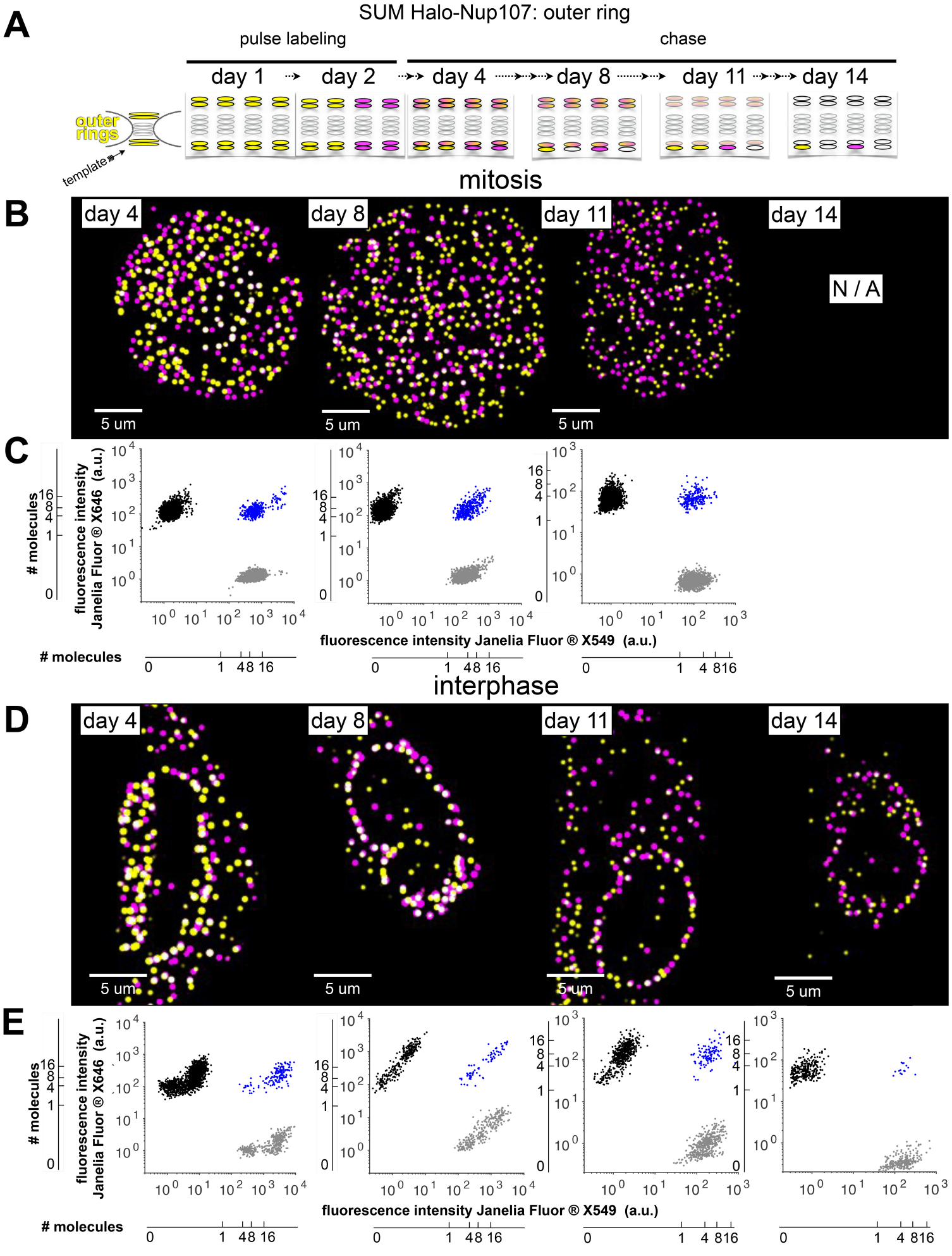
A
SUM Halo-Nup107: outer ring
pulse labeling
chase
day 1
day 2
day 4
day 8
day 11
day 14
outer rings
template
mitosis
B
day 4
day 8
day 11
day 14
N / A
5 um
5 um
5 um
C
molecules
fluorescence intensity Janelia Fluor ® X646 (a.u.)
fluorescence intensity Janelia Fluor ® X549 (a.u.)
molecules
interphase
D
day 4
day 8
day 11
day 14
5 um
5 um
5 um
5 um
E
molecules
fluorescence intensity Janelia Fluor ® X646 (a.u.)
fluorescence intensity Janelia Fluor ® X549 (a.u.)
molecules

Figure S7. Inheritance during mitosis and interphase of outer ring subassemblies containing Nup107, Related to Figures 2 and S8.

(A) Schematic representation of pulse-chase experiments in which asynchronous populations of genome-edited SUM159 cells expressing Halo-Nup107 were subjected to brief incubation with Janelia Fluor ® X549 (yellow) on the first day, with Janelia Fluor ® X646 (magenta) on the second day, and visualized volumetrically on days 4, 11 and 14 by LLSM after chemical fixation; the models follow the observed inheritance of outer ring subassemblies and the stochastic incorporation of monomeric Nup107 (as part of the Y-complex) as they incorporate back into NPCs imaged during interphase in consecutive days.

(B,D) The images correspond to approximately equatorial single-plane 2D views after 3D localization from z-scans acquired with LLSM from cells, chemically fixed during prometaphase or interphase on the indicated days after the first labeling following the steps described in (E). Scale bars, 5 um.

(C, E) The log-log plots show results for all detected spots in the complete volume of typically 2-3 per conditions indicated in panels (B,D). They show the maximum amplitude fluorescence intensity of HaloTag ligands on the spots determined from the corresponding Gaussian fits and the local background. Fluorescent spots were considered colocalized if their fitted positions were within 300 nm laterally, and 500 nm axially.The number of HaloTag ligand molecules on a diffraction-limited spot was calculated as the ratio between the starting fluorescence amplitude (before bleaching) and the bleaching step size determined for each acquisition.

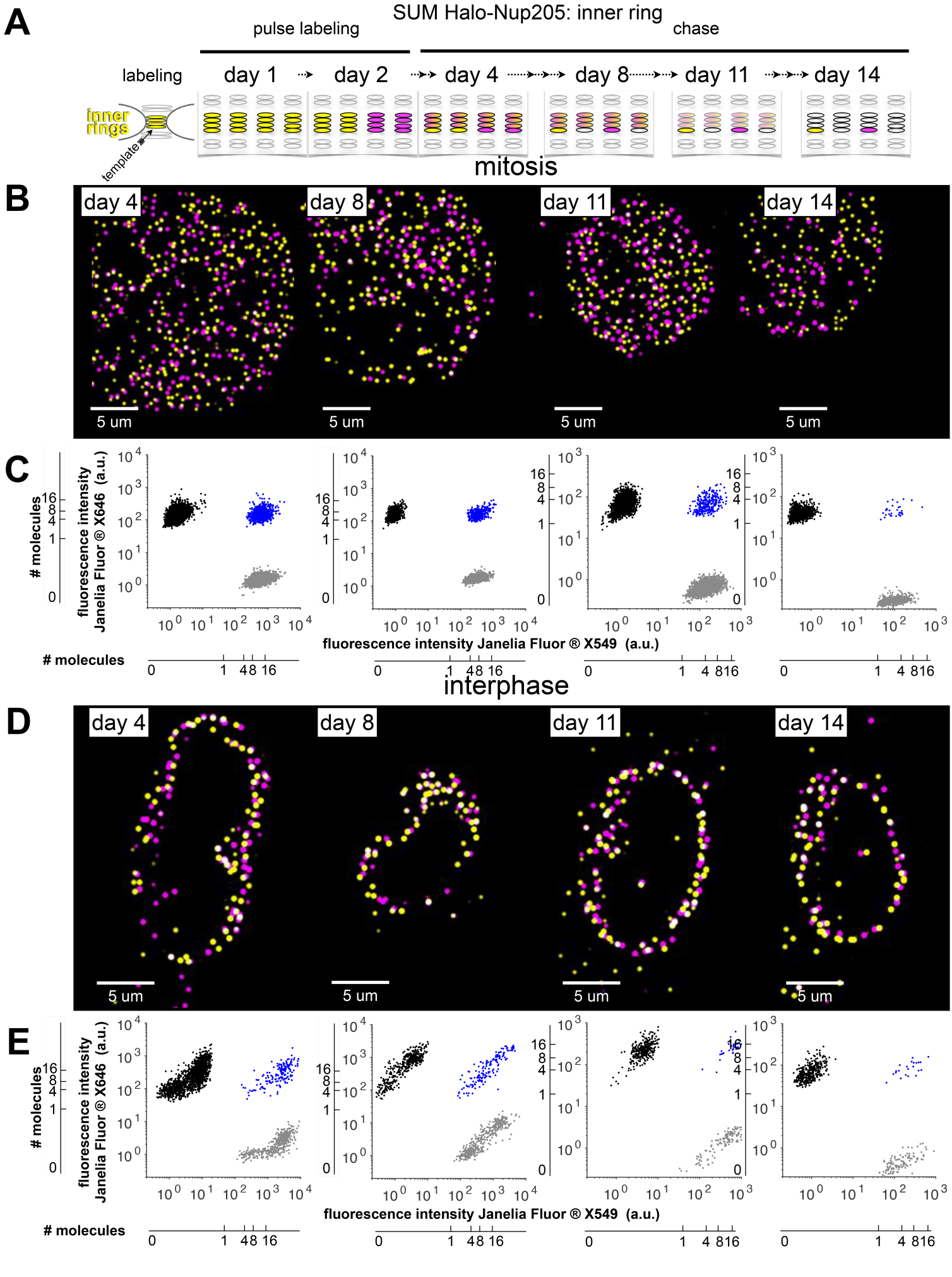
A
SUM Halo-Nup205: inner ring
pulse labeling
chase
labeling
day 1
day 2
day 4
day 8
day 11
day 14
inner rings
template
mitosis
B
day 4
day 8
day 11
day 14
5 um
C
molecules
fluorescence intensity Janelia Fluor ® X646 (a.u.)
fluorescence intensity Janelia Fluor ® X549 (a.u.)
interphase
D
E

Figure S8. Inheritance during mitosis and interphase of outer ring subassemblies containing Nup205, Related to Figures 2 and S7.

(A) Schematic representation of pulse-chase experiments in which asynchronous populations of genome-edited SUM159 cells expressing Halo-Nup205 were subjected to brief incubation with Janelia Fluor ® X549 (yellow) on the first day, with Janelia Fluor ® X646 (magenta) on the second day, and visualized volumetrically on days 4, 8, 11 and 14 by LLSM after chemical fixation; the models follow the observed inheritance of inner ring subassemblies and the stochastic incorporation of monomeric Nup205 as they incorporate back into NPCs imaged during interphase in consecutive days.

(B,D) The images correspond to approximately equatorial single-plane 2D views after 3D localization from z-scans acquired with LLSM from cells, chemically fixed during prometaphase or interphase on the indicated days after the first labeling following the steps described in (E). Scale bars, 5 um.

(C,E) The log-log plots show results for all detected spots in the complete volume of typically 2-3 per conditions indicated in panels (B,D). They show the maximum amplitude fluorescence intensity of HaloTag ligands on the spots determined from the corresponding Gaussian fits and the local background. Fluorescent spots were considered colocalized if their fitted positions were within 300 nm laterally, and 500 nm axially. The number of HaloTag ligand molecules on a diffraction-limited spot was calculated as the ratio between the starting fluorescence amplitude (before bleaching) and the bleaching step size determined for each acquisition.

Table S1. Number of diffraction-limited fluorescent spots detected in mitotic and interphase cells during consecutive days of cell division, Related to Figures 2, S7 and S8. The table summarizes the data used to generate the log-log plots from the results of pulse-chase experiments shown in Figs. S7E and S8 E. Fluorescent spots were considered colocalized if their fitted positions were within 300 nm laterally, and 500 nm axially.

Number of diffraction-limited fluorescent spots detected in mitotic and interphase cells of pulse-chase experiments shown in Figs. S7 and S8

Cell/Day	4	8	11	14
mito107	2	2	4	0
inter107	6	3	5	5
mito205	4	1	4	3
inter205	7	6	4	5
	19	12	17	13

day4

mito107

cell	colocalization	only X549	only X646
1	143	878	1145
2	206	1128	1282
Total	349	2006	2427

inter107

cell	colocalization	only X549	only X646
1	19	39	258
2	48	82	289
3	35	135	463
4	18	35	200
5	14	38	234
6	23	62	251
Total	157	391	1695

mito205

cell	colocalization	only X549	only X646
1	220	1018	1120
2	87	486	485
3	351	1754	1805
4	159	777	1045
Total	817	4035	4455

inter205

cell	colocalization	only X549	only X646
1	24	64	248
2	32	70	274
3	14	30	236
4	19	64	169
5	54	129	335
6	17	55	184
7	16	57	162
Total	176	469	1608

day8

mito107

cell	colocalization	only X549	only X646
1	268	1489	1634
2	69	398	610
Total	337	1887	2244

inter107

cell	colocalization	only X549	only X646
1	28	93	72
2	16	60	78
3	30	126	136
Total	74	279	286

mito205

cell	colocalization	only X549	only X646
1	321	1648	1014
Total	321	1648	1014

inter205

cell	colocalization	only X549	only X646
1	69	132	116
2	37	102	83
3	6	34	55
4	21	41	75
5	26	67	50
6	3	17	27
Total	162	393	406

day11

mito107

cell	colocalization	only X549	only X646
1	45	524	757
2	86	745	691
3	39	362	314
4	54	481	436
Total	131	1269	1448

inter107

cell	colocalization	only X549	only X646
1	3	96	129
2	5	73	86
3	66	109	153
4	21	77	80
5	11	91	82
Total	106	446	530

mito205

cell	colocalization	only X549	only X646
1	28	409	342
2	59	399	575
3	83	858	735
4	84	784	726
Total	254	2450	2378

inter205

cell	colocalization	only X549	only X646
1	13	28	146
2	8	36	40
3	19	65	106
Total	40	129	292

day14

inter107

cell	colocalization	only X549	only X646
1	3	50	39
2	2	35	57
3	1	30	28
4	2	42	65
5	7	99	78
Total	15	256	267

mito205

cell	colocalization	only X549	only X646
1	11	285	105
2	17	230	346
3	5	161	330
Total	33	676	781

inter205

cell	colocalization	only X549	only X646
1	7	30	75
2	10	37	158
3	1	15	57
4	1	6	25
5	3	30	32
6			
Total	22	118	347